

Uplink HARQ for Distributed and Cloud RAN via Separation of Control and Data Planes

Shahrouz Khalili, *Student Member, IEEE* and Osvaldo Simeone, *Fellow, IEEE*

Abstract

The implementation of uplink HARQ in a Distributed-Radio Access Network (D-RAN) or Cloud-RAN (C-RAN) architecture is constrained by the two-way latency on the fronthaul links connecting the Remote Radio Heads (RRHs) with the Baseband Units (BBUs) that perform decoding. To overcome this limitation, this work considers an architecture based on the separation of control and data planes, in which retransmission decisions are made at the edge of the network, that is, by the RRHs or User Equipments (UEs), while data decoding is carried out remotely at the BBUs. This architecture enables *low-latency local retransmission decisions* to be made at the RRHs or UEs, which are not subject to the fronthaul latency constraints, while at the same time leveraging the decoding capability of the BBUs. A D-RAN system is first considered in which *low-latency local feedback* from the RRH assigned to a given UE is used to drive the UE's HARQ process. Throughput and probability of error of this solution are analyzed for the three standard HARQ modes of Type-I, Chase Combining and Incremental Redundancy over a general fading MIMO link. Then, novel *user-centric low-latency feedback* strategies are proposed and analyzed for the C-RAN architecture based on limited “hard” or “soft” local feedback from the RRHs to the UE and on retransmission decisions taken at the UE. The analysis presented in this work allows the optimization of the considered schemes, as well as the investigation of the impact of system parameters such as HARQ protocol type, blocklength and number of antennas on the performance of low-latency local HARQ decisions in D-RAN and C-RAN architectures.

Index Terms

D-RAN, C-RAN, HARQ, Throughput, MIMO, Chase Combining, Incremental Redundancy, Control and Data Planes Separation Architecture.

This work was partially supported by the U.S. NSF grant CCF-1525629.

S. Khalili and O. Simeone are with CWCSPP, ECE Dept, NJIT, Newark, USA. E-mail: {sk669, osvaldo.simeone}@njit.edu.

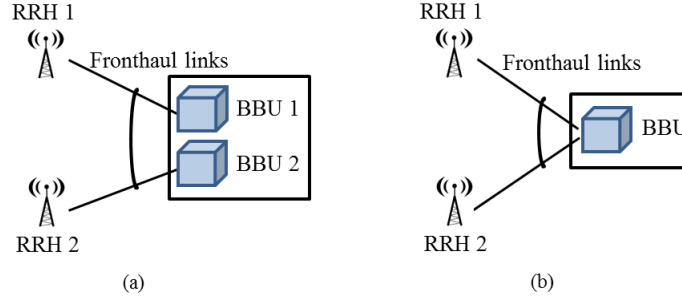


Fig. 1. Illustration of the (a) D-RAN and (b) C-RAN architecture ($L = 2$ RRHs).

I. INTRODUCTION

Distributed and Cloud Radio Access Network, abbreviated as D-RAN and C-RAN, respectively, are candidate cellular architectures for 5G systems, in which the baseband processing unit (BBU) of each base station is virtualized at a “cloud” processor. This virtualization yields the separation between the remote radio head (RRH) that implements the radio functionalities of the base station and a centralized BBU that is charged with higher-layer tasks, including the physical layer.

In a D-RAN, as seen in Fig. 1-(a), the BBU of each base station is hosted at a remote site, which is accessed by the RRH via connections known as *fronthaul* links. In a D-RAN, the BBUs of different RRHs are hence distinct. The D-RAN architecture lowers the expenditure needed to deploy and operate dense cellular networks, by simplifying the base stations hardware and by enabling flexible upgrading and easier maintenance (see, e.g., [1]–[3]). D-RAN also allows limited forms of cooperation to be implemented among base stations, particularly in the downlink, by leveraging an X2 interface that may connect the BBUs with one another within the same “cloud” [3]. Nevertheless, joint baseband decoding in the uplink is generally not feasible in a D-RAN, since it requires the exchange of baseband signals among BBUs, rather than user-plane data as allowed by an X2 interface (see e.g., [1]–[3]). Therefore, a D-RAN operates as a conventional cellular system, in which each user equipment (UE) is assigned to one RRH.

In a C-RAN architecture, instead, a unique BBU is shared among multiple RRHs, as depicted in Fig. 1-(b). Therefore, C-RAN enables joint baseband processing across all the RRHs connected to the same BBU. In addition to the gains achieved by D-RAN, C-RAN can hence also benefit from the statistical multiplexing and interference management capabilities that are made possible by joint baseband processing across multiple RRHs. Furthermore, no UE-RRH assignment is

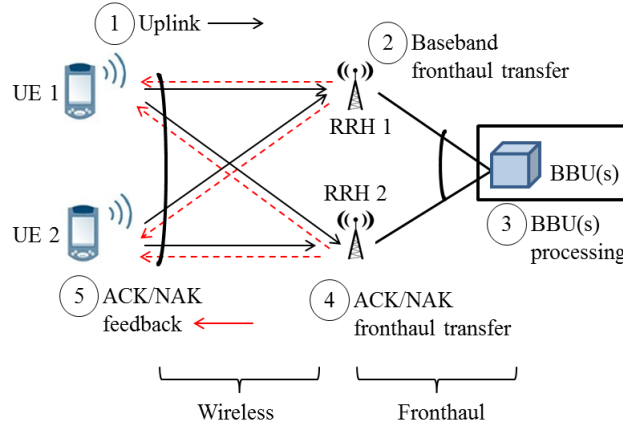


Fig. 2. Conventional HARQ in D-RAN or C-RAN. The numbers indicate the sequence of events associated with a transmission. Fronthaul latency is associated with the fronthaul transmissions at steps 2 and 4 and with the part of BBU processing at step 3 needed to encode and decode transmissions on the fronthaul links. The cross-links in the uplink carry interference in a D-RAN and useful signals in a C-RAN. The dashed cross-links in the ACK/NAK feedback path are used only in the C-RAN architecture.

necessary (see, e.g., [1], [2]).

Main Problem: The implementation of the D-RAN and C-RAN architectures needs to contend with the potentially significant latencies needed for the transfer and processing of the baseband signals on the fronthaul links to and from the BBU(s) [4]. The communication protocols that are most directly affected by fronthaul delays are the Automatic Repeat Request (ARQ) and Hybrid ARQ (HARQ)¹ protocols at layer 2 of the protocol stack. In fact, in a conventional cellular network, upon receiving a codeword from an UE, the local base station performs decoding, and, depending on the decoding outcome, feeds back an Acknowledgment (ACK) or a Negative Acknowledgment (NAK) to the UE. In contrast, in a D-RAN or C-RAN, as illustrated in Fig. 2, the outcome of decoding at the BBU may only become available at the RRHs after the time required for the transfer of the baseband signals from the RRHs to the BBU(s) on the fronthaul links, for processing at the BBU(s), and for the transmission of the decoding outcome from the BBU(s) to the RRHs on the fronthaul links.

The fronthaul latency may significantly affect the performance of retransmission protocols. For instance, in LTE with frequency division multiplexing, the feedback latency should be less

¹In ARQ protocols, different transmissions of a packet are performed independently, whereas, in HARQ schemes, decoding and/or coding can be performed across multiple retransmissions [5].

than 3 ms in order not to disrupt the operation of the system [6]². We also refer to [7] for a discussion on the effect of the latency on ARQ protocols in C-RANs.

A Solution Based on the Separation of Control and Data Planes: Fronthaul latency is unavoidable in conventional D-RAN and C-RAN architectures in which the RRHs only retain radio functionalities. Nevertheless, alternative functional splits are currently being investigated whereby the RRH may implement some additional functions [2], [6], [8], [9]. In this work, we consider a functional split that enables the *separation of control and data planes associated with the HARQ protocol*, with the aim of alleviating the problem of fronthaul latency. We note that the approach studied here can be seen as an instance of the more general principle of control and data separation, for which an overview of the literature can be found in [10].

In particular, we investigate an architecture in which retransmission decisions are made at the edge of the network, that is, by the RRHs or UEs, while data decoding is carried out remotely at the BBUs as in a conventional D-RAN or C-RAN. This architecture enables *low-latency local retransmission decisions* to be made at the RRHs or UEs, which are not subject to the fronthaul latency constraints, while at the same time leveraging the decoding capability of the BBUs.

Low-latency local control of the retransmission process is made possible by an RRH-BBU functional split whereby each RRH can perform synchronization and resource demapping, so as to distinguish the different fields of a frame [6]³. In fact, this functional split allows the RRHs to gather information about the modulation and coding scheme (MCS) used in the uplink packet, as well as on the channel state information (CSI) about the local uplink channels. As proposed in [6] and in [11], for a D-RAN system, based on the available MCS and CSI, the RRH assigned to a UE can make local decisions about whether successful or unsuccessful decoding is expected to occur at the BBU, feeding back an ACK/NAK message to the UE accordingly. The RRH associated to a UE makes this *local low-latency feedback decision* without waiting to be notified about the actual decoding outcome at the BBU and without running the channel decoder, which is implemented only at the BBU. Fig. 4 presents an illustration of the outlined low-latency approach.

²By interleaving multiple HARQ processes, as discussed in [6], the tolerated latency can be increased to $3 + n8$ ms, where n is a positive integer, albeit at the cost of possibly reducing the throughput. Of the mentioned 3 ms latency, it has been recently specified that the one-way transport delay on the fronthaul should be no larger than around 400 μ s [4].

³In an OFDM system, such as LTE, this requires also the implementation of an FFT block.

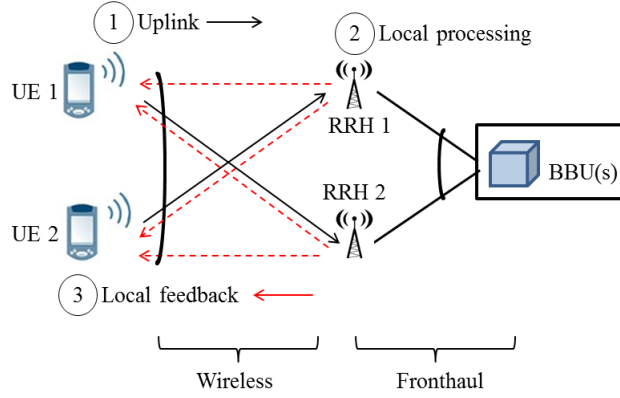


Fig. 3. HARQ in D-RAN and C-RAN systems via low-latency local feedback based on separation of control and data planes. HARQ control is carried out at the network edge based on local low-latency feedback from the RRHs, while data decoding is carried out at the BBUs. The cross-links in the uplink carry interference in a D-RAN and useful signals in a C-RAN. The cross-links in the feedback path are used only in the C-RAN architecture.

The local feedback approach under discussion introduces possible errors due to the mismatch between the local decision at the RRH and the actual decoding outcome at the BBU. Indeed, the RRH may request an additional retransmissions for a packet that the BBU is able to decode, or acknowledge correct reception of a packet for which decoding eventually fails at the BBU, hence causing a throughput degradation.

In a C-RAN, which is characterized by joint baseband processing across multiple RRHs, the outlined approach based on local feedback is complicated by the fact that the channel state information between the UE and each RRH is not known to other RRHs. Therefore, it is not possible for the RRHs to directly agree on HARQ control decisions, making the local feedback mechanism proposed in [6] and [11] not applicable.

Main contributions: The main contributions of this paper are summarized as follows.

- For D-RAN, we analyze throughput and probability of error of low-latency local feedback for the three standard HARQ modes of Type-I (TI), Chase Combining (CC) and Incremental Redundancy (IR) over a multi-antenna, or MIMO, link with coding blocks (packets) of arbitrary finite length. This is done by leveraging recently derived finite-blocklength tight capacity bounds [12]. As a result, unlike the existing literature [6] and [11], the analysis allows the investigation of the impact of system parameters such as HARQ protocol type, blocklength and number of antennas. We note that the analysis in [11] focuses on the throughput of single-antenna links in a D-RAN with HARQ-IR and is based on an

error exponent framework, which is known to provide an inaccurate evaluation of the probability of error in the practical finite-blocklength regime [12, Eq. (54)] [13, Sec. 1.2 and Sec. 1.3].

- We propose and analyze *user-centric low-latency feedback* schemes for C-RAN systems. According to these proposed techniques, limited-feedback information is sent from each RRH to an UE in order to allow the latter to make a low-latency local control decision about the need for a retransmission. A “hard feedback” approach is first proposed that directly generalizes the D-RAN scheme described above and requires a one-bit feedback message from each RRH. Then, a “soft feedback” strategy is proposed in which the UE decision is based on multi-bit feedback from the RRHs, consisting of quantized local CSI.

The rest of the paper is organized as follows. In Sec. II, the system model for D-RAN and C-RAN systems is introduced. Sec. III details the principles underlying the proposed low-latency local feedback solutions for D-RAN and C-RAN. The metrics used to evaluate the performance of the proposed schemes and some preliminaries are discussed in Sec. IV. In Sec. V and Sec. VI, the analysis of D-RAN and C-RAN strategies is presented. In Sec. VII, the numerical results are provided, and Sec. VIII concludes the paper.

Notation: Bold letters denote matrices and superscript H denote Hermitian conjugation. $\mathcal{CN}(\mu, \sigma^2)$ denotes a complex normal distribution with mean μ and variance σ^2 ; and \mathcal{X}_k^2 a Chi-Squared distribution with k degrees of freedom. $f_{\mathcal{A}}(x)$ and $F_{\mathcal{A}}(x)$ represent the probability density function and the cumulative distribution function of a distribution \mathcal{A} evaluated at x , respectively. $\mathbf{A} = \text{diag}([\mathbf{A}_1, \dots, \mathbf{A}_n])$ is a block diagonal matrix with block diagonal given by the matrices $[\mathbf{A}_1, \dots, \mathbf{A}_n]$. The indicator function $\mathbf{1}(x)$ equals 1 if $x = \text{true}$ and 0 if $x = \text{false}$.

II. SYSTEM MODEL

We study the uplink of both D-RAN and C-RAN systems as illustrated in Fig. 1. In this section, we detail system model and performance metrics.

A. System Model

As seen in Fig. 1, each RRH is connected by means of orthogonal fronthaul links to a dedicated BBU for D-RAN and to a single BBU for C-RAN systems. The BBUs perform decoding, while the RRHs have limited baseband processing functionalities that allow resource demapping and the inference of CSI and MCS information as discussed in Sec. I and further detailed below.

Different UEs are served in distinct time-frequency resources, as done for instance in LTE, and hence we focus here on the performance of a given UE.

Each packet transmitted by the UE contains k encoded complex symbols and is transmitted within a coherence time/frequency interval of the channel, which is referred to as *slot*. The transmission rate of the first transmission of an information message is defined as r bits per symbol, so that kr is the number of information bits in the information message.

Each transmitted packet is acknowledged via the transmission of a feedback message by the RRHs. We assume that these feedback messages are correctly decoded by the UE. We will first assume that messages are limited to binary positive or negative acknowledgments, i.e., ACK or NAK messages, in Sec. III-A, and we will consider the more general case in which feedback messages may consist of $b \geq 1$ bits in Sec. III-B. The same information message may be transmitted for up to n_{max} successive slots using standard HARQ protocols such as TI, CC and IR, to be recalled in Sec. III.

The UE is equipped with m_t transmitting antennas, while $m_{r,l}$ receiving antennas are available at the l th RRH. The received signal for any n th slot at the l th RRH can be expressed as

$$\mathbf{y}_{l,n} = \sqrt{\frac{s}{m_t}} \mathbf{H}_{l,n} \mathbf{x}_n + \mathbf{w}_{l,n}, \quad (1)$$

where s measures the average SNR per receive antenna; $\mathbf{x}_n \in \mathbb{C}^{m_t \times 1}$ represents the symbols sent by the transmit antennas at a given channel use, whose average power is normalized as $\mathbb{E}[\|\mathbf{x}_n\|^2] = 1$; $\mathbf{H}_{l,n} \in \mathbb{C}^{m_{r,l} \times m_t}$ is the channel matrix, which is assumed to have independent identically distributed (i.i.d.) $\mathcal{CN}(0, 1)$ entries (Rayleigh fading); and $\mathbf{w}_{l,n} \in \mathbb{C}^{m_{r,l} \times 1}$ is an i.i.d. Gaussian noise vector with $\mathcal{CN}(0, 1)$ entries. The channel matrix $\mathbf{H}_{l,n}$ are independent for different RRHs $l \in \{1, \dots, L\}$ and also change independently in each slot n . Moreover, they are assumed to be known to the l th RRH and to the BBU. We assume the use of Gaussian codebooks with an equal power allocation across the transmit antennas, although the analysis could be extended to arbitrary power allocation and antenna selection schemes.

B. Performance Metrics

The main performance metrics of interest are as follows.

- Throughput T : The throughput measures the average rate, in bits per symbol, at which information can be successfully delivered from the UE to the BBU;

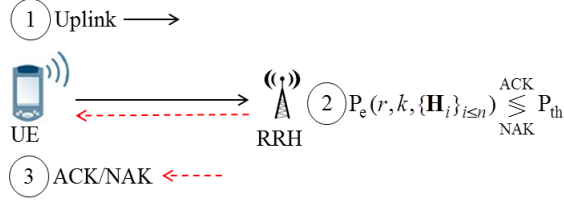


Fig. 4. Low-latency local feedback scheme for D-RAN systems: ACK/NAK messages are sent by the assigned RRH to a given UE according to the local decision rule (2).

- **Probability P_s of success:** The metric P_s measures the probability of a successful transmission within a given HARQ session, which is the event that, in one of the n_{max} allowed transmission attempts, the information message is decoded successfully at the BBU.

Note that errors in the HARQ sessions can be dealt with by higher layers, as done by the RLC layer in LTE [6], albeit at the cost of large delays. For this reason, in Sec. VII, we will pay special attention to the throughput that can be obtained under a given constraint on the probability of success P_s . Typical values for P_s , on which one can base the design of higher layers, are in the order of 0.99 – 0.999 [3] [14]. We elaborate on the evaluation of these metrics in Sec. IV.

III. LOW-LATENCY LOCAL FEEDBACK

In this section, we introduce the key working principles underlying low-latency local feedback solutions for D-RAN and C-RAN.

A. RRH-Based Low-Latency Local Feedback for D-RAN

In a D-RAN architecture, each pair of RRH and corresponding BBU operates as a base station in a conventional cellular system [1] [2]. Therefore, an UE is assigned to a specific RRH-BBU pair by following standard user association rules. For D-RAN, as in [11], we can then focus on a single RRH, i.e., $L = 1$, with the understanding that the noise term in (1) may account also for the interference from UEs associated to other RRH-BBU pairs. When studying D-RAN systems, we hence drop the subscript l indicating the RRH index.

The low-latency local feedback scheme for D-RAN, first proposed in [6], is illustrated in Fig. 4. At each transmission attempt n , the RRH performs resource demapping and obtains CSI about the channel \mathbf{H}_n and the MCS used for data transmission. The MCS amounts here to the rate r and packet length k . Based on this information, the RRH can compute the probability of

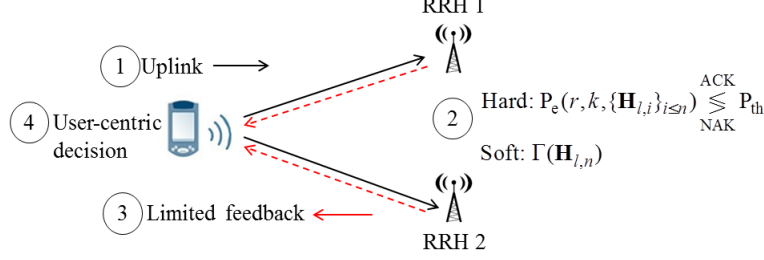


Fig. 5. Low-latency local feedback scheme for C-RAN systems: The UE collects limited-feedback messages from the RRHs to make a local decision on whether another transmission attempt is necessary.

error $P_e(r, k, \{\mathbf{H}_i\}_{i \leq n})$ for decoding at the BBU, where we emphasized the possible dependence of the probability of error P_e on all channel matrices $[\mathbf{H}_1, \dots, \mathbf{H}_n]$ corresponding to prior and current transmission attempts. We note that the probability P_e may be read on a look-up table or obtained from some analytical approximations as discussed in the next section. As proposed in [11], if the decoding error probability $P_e(r, k, \{\mathbf{H}_i\}_{i \leq n})$ is smaller than a given threshold P_{th} , the RRH sends an ACK message to the UE, predicting a positive decoding event at the BBU; while, otherwise, a NAK message is transmitted, that is,

$$P_e(r, k, \{\mathbf{H}_i\}_{i \leq n}) \underset{\text{NAK}}{\overset{\text{ACK}}{\leq}} P_{th}. \quad (2)$$

As we will discuss in Sec. VII, the optimization of the threshold P_{th} needs to strike a balance between the probability of success P_s , which would call for a smaller P_{th} and hence more retransmissions, and the throughput T , which may be generally improved by a larger P_{th} , resulting in the transmission of new information.

B. User-Centric Low-Latency Local Feedback for C-RAN

In C-RAN, unlike D-RAN systems, a BBU jointly processes the signals received by several connected RRHs (Fig. 1-(b)). Therefore, a UE-RRH assignment step is not needed as the BBU performs decoding based on the signals received from all connected RRHs. The development of a local feedback solution for C-RAN is hence complicated by the fact that the BBU decoding error probability $P_e(r, k, \{\mathbf{H}_i\}_{i \leq n})$ depends on the CSI $\{\mathbf{H}_i\}_{i \leq n}$ between the UE and all RRHs, while each RRH l is only aware of the CSI $\{\mathbf{H}_{l,i}\}_{i \leq n}$ between the UE and itself. Therefore, the decoding error probability $P_e(r, k, \{\mathbf{H}_i\}_{i \leq n})$ cannot be calculated at any RRH as instead done for D-RAN.

To overcome this problem, in this paper, we propose a user-centric low-latency local HARQ mechanism, whereby the UE collects limited-feedback messages from the RRHs, based on which it makes a local decision about whether a further retransmission attempt is needed or not, illustrated in Fig. 5. We allow for multi-bit feedback messages from the RRHs to the UE, and study methods based on *hard feedback*, and *soft feedback*, as explained next.

1) *Hard Feedback*: The hard feedback scheme is a direct extension of the local feedback solution explained in Sec. III-A for D-RAN. Since at the n th transmission attempt, the l th RRH is only aware of the CSI $\{\mathbf{H}_{l,i}\}_{i \leq n}$ between itself and the UE, it can only calculate the decoding error probability $P_e(r, k, \{\mathbf{H}_{l,n}\}_{i \leq n})$, which corresponds to a scenario in which the BBU decodes solely based on the signal received by the l th RRH. Then, each RRH l uses a 1-bit quantizer, which maps the probability $P_e(r, k, \{\mathbf{H}_{l,n}\}_{i \leq n})$ to an ACK/NAK message according to the same rule used in D-RAN system, i.e.,

$$P_e(r, k, \{\mathbf{H}_{l,n}\}_{i \leq n}) \underset{\text{NAK}}{\overset{\text{ACK}}{\leq}} P_{\text{th}}. \quad (3)$$

The UE decides to retransmit the packet if all RRHs return a NAK message and to stop retransmissions if at least one ACK is received.

2) *Soft Feedback*: The soft feedback schemes aims at leveraging multi-bit feedback messages, composed of $b \geq 1$ bits, from each RRH to the UE. The key idea here is that the UE can estimate the decoding error probability $P_e(r, k, \{\mathbf{H}_i\}_{i \leq n})$ of the BBU upon receiving information from each RRH l about the local CSI $\mathbf{H}_{l,n}$. To this end, in the soft feedback scheme, each RRH quantizes its own CSI $\mathbf{H}_{l,n}$ by using vector quantization [15] with b bits and sends the quantized CSI $\Gamma(\mathbf{H}_{l,n}) = \hat{\mathbf{H}}_{l,n}$ to the UE via a b -bit feedback message. Then, the UE performs a retransmission if the estimated decoding error probability $P_e(r, k, \{\hat{\mathbf{H}}_i\}_{i \leq n})$, with $\hat{\mathbf{H}}_i$ collecting all the quantized matrices $\hat{\mathbf{H}}_{l,n}$ for $l \in \{1, \dots, L\}$, is larger than a threshold P_{th} and stop retransmission otherwise, as in

$$P_e(r, k, \{\hat{\mathbf{H}}_i\}_{i \leq n}) \underset{\text{NAK}}{\overset{\text{ACK}}{\leq}} P_{\text{th}}. \quad (4)$$

IV. PERFORMANCE CRITERIA AND PRELIMINARIES

In this section, we discuss the general approach that will be followed to evaluate throughput and probability of success for the considered schemes in D-RAN and C-RAN systems.

TABLE I. Error types due to low-latency local feedback

BBU decoding outcome	Local feedback decision	Consequence
Undecodable	STOP	Delays due to higher-layer protocols
Decodable	RTX	HARQ retransmission

A. Throughput and Probability of Success

To start, let us denote as RTX_n the event that a retransmission decision is made for all the first n transmission attempts of an information message. In a similar manner, we define as STOP_n the event that a decision is made to stop the retransmission of a packet at the n th attempt, and hence $n - 1$ retransmission attempts have been performed before. As we discussed in Sec. III, these decisions are made at the RRH for the low-latency local feedback scheme in D-RAN and at the UE in the proposed user-centric low-latency strategies for C-RAN. By definition, the probabilities of these events satisfy the equality

$$P(\text{STOP}_n) = P(\text{RTX}_{n-1}) - P(\text{RTX}_n). \quad (5)$$

Remark: In case of ideal feedback from the BBU, a STOP/RTX event reflects correct/incorrect decoding at the BBU, whereas this is not the case for the local feedback schemes due to the possible mismatch between the RRHs' or users' decisions and the decoding outcome at the BBU. In particular, there are two types of error as summarized in Table I. In the first type of error, the transmitted packet is not decodable at the BBU, but a STOP decision is made by the local feedback scheme. This type of mismatch needs to be dealt with by higher layers, introducing significant delays. In the second type of error, the received packet is decodable at the BBU, but an RTX decision is made. In this case, the UE performs an unnecessary retransmission. We observe that the first type of error is more deleterious to the performance as it affects directly the probability of success. ■

We now elaborate on the calculation of the throughput T and probability of success P_s for both the local feedback schemes and reference ideal case of zero-delay feedback from the BBU. For all schemes, based on standard renewal theory arguments, the throughput can be calculated as [16]

$$T = \frac{rP_s}{E[N]}, \quad (6)$$

where we recall that r is the transmission rate, and the random variable N denotes the number of transmission attempts for a given information message. The average number of transmissions can be computed directly as

$$E[N] = \sum_{n=1}^{n_{max}-1} nP(\text{STOP}_n) + n_{max}P(\text{RTX}_{n_{max}-1}). \quad (7)$$

Moreover, the probability of a successful transmission for the case of zero-delay feedback from the BBU is given as

$$P_s = 1 - P(\text{RTX}_{n_{max}}). \quad (8)$$

Instead, with local feedback, a transmission is considered as successful if a decision is made to stop the retransmission of a packet within one of the n_{max} allowed transmissions attempts *and* if the BBU can correctly decode. Hence, by the law of total probability, the probability of success P_s can be written as

$$P_s = \sum_{n=1}^{n_{max}} P(D_n|\text{STOP}_n)P(\text{STOP}_n), \quad (9)$$

where D_n is the event that the BBU can correctly decode at the n th transmission.

In summary, in order to evaluate the throughput, we use (5)-(7) for both ideal and local feedback; while, for the probability of success P_s , we use (8) for the case of ideal feedback and (9) for local feedback. Therefore, to compute both metrics, we only need to calculate the probabilities $P(\text{RTX}_n)$, for both ideal and local feedback, and the probabilities $P(D_n|\text{STOP}_n)$ for local feedback, with $n = 1, \dots, n_{max}$. We will use this approach in the next two sections for D-RAN and C-RAN systems.

B. Gaussian Approximation

Throughout this paper, we adopt the Gaussian approximation proposed in [17], based on the work in [12], to evaluate the probability $P_e(r, k, \mathbf{H})$ of decoding error for a transmission at rate r in a slot of k channel uses when the channel matrix is \mathbf{H} . This amounts to

$$P_e(r, k, \mathbf{H}) = Q\left(\frac{C(\mathbf{H}) - r}{\sqrt{\frac{V(\mathbf{H})}{k}}}\right), \quad (10)$$

where we have defined

$$C(\mathbf{H}) = \sum_{j=1}^{m_{rt}} \log_2 \left(1 + \frac{s\lambda_j}{m_t}\right) \text{ and } V(\mathbf{H}) = \left(m_{rt} - \sum_{j=1}^{m_{rt}} \frac{1}{\left(1 + \frac{s\lambda_j}{m_t}\right)^2}\right) \log_2^2 e, \quad (11)$$

with $m_{rt} = \min(m_r, m_t)$; $\{\lambda_j\}_{j=1, \dots, m_{rt}}$ being the eigenvalues of the matrix $\mathbf{H}^H \mathbf{H}$; and $Q(\cdot)$ being the Gaussian complementary cumulative distribution function. Expressions obtained by means of the Gaussian approximation (10) will be marked for simplicity of notation as equalities in the following.

For future reference, we note that we have the limit

$$\lim_{k \rightarrow \infty} P_e(r, k, \mathbf{H}) = \begin{cases} 1 & \text{if } C(\mathbf{H}) < r \\ 0 & \text{if } C(\mathbf{H}) > r \end{cases} \quad (12)$$

in the asymptotic regime of large blocklengths.

V. ANALYSIS OF RRH-BASED LOW-LATENCY LOCAL FEEDBACK FOR D-RAN

In this section, we analyze the performance in terms of throughput and probability of success of the low-latency local feedback scheme for D-RAN introduced in Sec. III-A. We focus separately on the three standard modes of HARQ-TI, CC and IR, in order of complexity [18]. We recall that, in the considered low-latency scheme, a decision to stop retransmissions is made by the RRH by sending an ACK message, while a retransmission is decided by the transmission of a NAK message. We define as ACK_n the event that an ACK message is sent at the n th transmission attempt and as NAK_n the event that a NAK message is sent for all the first n transmissions. Therefore, in applying the analytical expression introduced in the previous section, we can focus on the evaluation of the probabilities $P(\text{RTX}_n) = P(\text{NAK}_n)$ and $P(D_n | \text{STOP}_n) = P(D_n | \text{ACK}_n)$ in order to calculate throughput and probability of success. Throughout, we use the Gaussian approximation for the probability of error discussed in Sec. IV-B.

A. HARQ-TI

With HARQ-TI, the same packet is retransmitted by the UE upon reception of a NAK message until the maximum number n_{max} of retransmissions is reached or until an ACK message is received. Moreover, decoding at the BBU is based on the last received packet only. HARQ-TI is hence a standard ARQ strategy [5].

1) Ideal Feedback: For reference, we first study the ideal case in which zero-delay feedback is available directly from BBU. Using the approximation (10) and averaging over the channel distribution, the approximate probability of an erroneous decoding at the BBU at the n th re-

transmission is given by $E[P_e(r, k, \mathbf{H}_n)]$. Accordingly, since with HARQ-TI the BBU performs decoding independently for each slot, we obtain

$$P(\text{NAK}_n) = (E[P_e(r, k, \mathbf{H})])^n. \quad (13)$$

As discussed, throughput and the probability of success now can be calculated as (2)-(4) and (5), where the throughput can be simplified as

$$T = r(1 - E[P_e(r, k, \mathbf{H})]). \quad (14)$$

The average in (14) can be computed numerically based on the known distribution of the eigenvalues the Wishart-distributed matrix $\mathbf{H}^H \mathbf{H}$, see [19, Theorem 2.17]. As an important special case, for a SISO link ($m_t = m_r = 1$), we have $|H|^2 \sim \chi_2^2$ and hence

$$E[P_e(r, k, H)] = \int_0^\infty P_e(r, k, \sqrt{x}) f_{\chi_2^2}(x) dx. \quad (15)$$

2) *Local Feedback*: With local feedback, as discussed, at each transmission attempt n , the RRH estimates the current channel realization \mathbf{H}_n and decides whether it expects the BBU to decode correctly or not by comparing the probability of error by using the following rule (2), which reduces to

$$P_e(r, k, \mathbf{H}_n) \underset{\text{NAK}}{\overset{\text{ACK}}{\leq}} P_{\text{th}}, \quad (16)$$

since decoding is done only based on the last received packet. We observe that, in the case of a single antenna at the transmitter and/or the receiver, the rule (16) only requires the RRH to estimate the SNR $s||\mathbf{H}_n||^2/m_t$.

The quantities that are needed to calculate the performance metrics under study can be then directly obtained from their definitions as

$$P(D_n|\text{ACK}_n) = 1 - E[P_e(r, k, \mathbf{H}) | P_e(r, k, \mathbf{H}) \leq P_{\text{th}}] \quad (17)$$

$$\text{and } P(\text{NAK}_n) = (P(P_e(r, k, \mathbf{H}) > P_{\text{th}}))^n. \quad (18)$$

As discussed, (17) and (18) can be obtained by averaging over the distribution of the eigenvalues of $\mathbf{H}^H \mathbf{H}$. As an example, for a SISO link, we obtain

$$P(D_n|\text{ACK}_n) = 1 - \frac{1}{1 - F_{\chi_2^2}(\gamma(P_{\text{th}}))} \int_{\gamma(P_{\text{th}})}^\infty P_e(r, k, \sqrt{x}) f_{\chi_2^2}(x) dx \quad (19)$$

$$\text{and } P(\text{NAK}_n) = \left(F_{\chi_2^2}(\gamma(P_{\text{th}}))\right)^n, \quad (20)$$

where $\gamma(P_{\text{th}})$ is calculated by solving the non-linear equation

$$P_e(r, k, \sqrt{\gamma(P_{\text{th}})}) = P_{\text{th}}, \quad (21)$$

e.g., by means of bisection.

B. HARQ-CC

With HARQ-CC, every retransmission of the UE consists of the same encoded packet as for TI. However, at the n th transmission attempt, the BBU uses maximum ratio combining (MRC) of all the n received packets in order to improve the decoding performance. For HARQ-CC, we only consider here a SISO link. This is because MRC requires to compute the weighted sum of the received signals across multiple transmission attempts, where the weight is given by the corresponding scalar channel for a SISO link. Note that SIMO and MISO links could also be tackled in a similar way by considering weights obtained from the effective scalar channels, although we do not explicitly consider these cases in the paper. Due to MRC, at the n th retransmission, the received signal can be written as

$$\bar{y}_n = \frac{\sum_{i=1}^n H_i^* y_i}{\bar{S}_n}, \quad (22)$$

or equivalently as

$$\bar{y}_n = \bar{S}_n x + \bar{w}_n, \quad (23)$$

where y_n is the n th received packet, the noise \bar{w}_n is distributed as $\mathcal{CN}(0, 1)$ and the effective channel gain of the combined signal is given by $\bar{S}_n = \sqrt{\sum_{i=1}^n |H_i|^2}$.

1) *Ideal Feedback*: The probability that the BBU does not decode correctly when the effective SNR is \bar{S}_n^2 is given as $P_e(r, k, \bar{S}_n)$. Let \bar{D}_n denote the event that the n th transmission is not decoded correctly at the BBU. The probability of the event NAK_n is then given as $P(\text{NAK}_n) = P(\bigcap_{j=1}^n \bar{D}_j)$, which can be upper bounded, using the chain rule of probability, as

$$P(\text{NAK}_n) = P(\bar{D}_n) P(\bar{D}_{n-1} | \bar{D}_n) \cdots P\left(\bar{D}_1 | \bigcap_{j=2}^n \bar{D}_j\right) \leq P(\bar{D}_n) = E[P_e(r, k, \bar{S}_n)]. \quad (24)$$

The usefulness of the bound (24) for small values of k will be validated in Sec. VII by means of a comparison with Monte Carlo simulations. We also refer to [20] where the same bound is proposed as an accurate approximation of the probability of error for HARQ-CC. We note that the inequality (24) is asymptotically tight in the limit of a large blocklength, since the limit $P(\bar{D}_m | \bigcap_{j=m+1}^n \bar{D}_j) \rightarrow 1$ as $k \rightarrow \infty$ holds for a fixed r due to (12) and to the inequality $\bar{S}_n \geq \bar{S}_m$

for $n \geq m$. The usefulness of the bound (24) for small values of k will be validated in Sec. VII by means of a comparison with Monte Carlo simulations. Since the effective SNR is distributed as $\bar{S}_n^2 = \sum_{i=1}^n |H_i|^2 \sim \mathcal{X}_{2n}^2$, the bound (24) can be calculated as

$$P(\text{NAK}_n) \leq \int_0^\infty P_e(r, k, \sqrt{x}) f_{\mathcal{X}_{2n}^2}(x) dx. \quad (25)$$

2) *Local Feedback*: With local feedback, the RRH decision is made according to the rule $P_e(r, k, \bar{S}_n) \leq_{\text{NAK}}^{\text{ACK}} P_{\text{th}}$, for a threshold P_{th} to be optimized. Similar to (17) and (18), we can compute the probabilities

$$P(D_n | \text{ACK}_n) = 1 - E \left[P_e(r, k, \bar{S}_n) | \{P_e(r, k, \bar{S}_{n-1}) > P_{\text{th}}\} \cap \{P_e(r, k, \bar{S}_n) \leq P_{\text{th}}\} \right] \quad (26)$$

$$\text{and } P(\text{NAK}_n) = P[P_e(r, k, \bar{S}_n) > P_{\text{th}}]. \quad (27)$$

Note that in (26)-(27) we used the fact that, if the condition $P_e(r, k, \bar{S}_n) > P_{\text{th}}$ holds, then we also have the inequality $P_e(r, k, \bar{S}_i) > P_{\text{th}}$ for all the indices $i < n$ due to the monotonicity of the probability $P_e(r, k, \bar{S})$ as a function of \bar{S} . Furthermore, noting that we can write $\bar{S}_n^2 = \bar{S}_{n-1}^2 + |H_n|^2$, where $\bar{S}_{n-1}^2 \sim \mathcal{X}_{2n-2}^2$ and $|H_n|^2 \sim \mathcal{X}_2^2$ are independent, from (26) and (27), we have

$$\begin{aligned} P(D_n | \text{ACK}_n) &= 1 - E \left[P_e(r, k, \bar{S}_n) | \{ \bar{S}_{n-1}^2 < \gamma(P_{\text{th}}) \} \cap \{ \bar{S}_{n-1}^2 + |H_n|^2 \geq \gamma(P_{\text{th}}) \} \right] \\ &= 1 - \frac{1}{\Delta(\gamma(P_{\text{th}}))} \int_0^{\gamma(P_{\text{th}})} \int_{\gamma(P_{\text{th}})-y}^\infty P_e(r, k, \sqrt{x+y}) f_{\mathcal{X}_2^2}(x) f_{\mathcal{X}_{2n-2}^2}(y) dx dy \end{aligned} \quad (28)$$

$$\text{and } P(\text{NAK}_n) = F_{\mathcal{X}_{2n}^2}(\gamma(P_{\text{th}})),$$

where $\Delta(\gamma(P_{\text{th}}))$ is defined as

$$\Delta(\gamma(P_{\text{th}})) = \int_0^{\gamma(P_{\text{th}})} \int_{\gamma(P_{\text{th}})-y}^\infty f_{\mathcal{X}_2^2}(x) f_{\mathcal{X}_{2n-2}^2}(y) dx dy. \quad (29)$$

C. HARQ-IR

With HARQ-IR, the UE transmits new parity bits at each transmission attempt and the BBU performs decoding based on all the received packets.

1) *Ideal Feedback*: With HARQ-IR, a set of n transmission attempt for a given information messages can be treated as the transmission over n parallel channels (see, e.g., [16]), and hence the error probability at the n th transmission can be computed as $P_e(r, k, \mathcal{H}_n)$ where $\mathcal{H}_n = \text{diag}([\mathbf{H}_1, \dots, \mathbf{H}_n])$ [17]. Moreover, following the same argument as (24), the decoding error at the n th transmission can be upper bounded as

$$P(\text{NAK}_n) \leq P(\bar{D}_n) = E[P_e(r, k, \mathcal{H}_n)], \quad (30)$$

which is tight for large values of k due to (12). This can be computed using the known distribution of the eigenvalues of the matrices $\mathbf{H}_i^H \mathbf{H}_i$ and the independence of the matrices \mathbf{H}_i for $i = 1, \dots, n$. For instance in the SISO case, we get

$$P(\text{NAK}_n) \leq \int_0^\infty \cdots \int_0^\infty P_e(r, k, \text{diag}([\sqrt{x_1}, \dots, \sqrt{x_n}])) \prod_{i=1}^n f_{\chi_2^2}(x_i) dx_1 \cdots dx_n. \quad (31)$$

2) *Local Feedback*: With local feedback, at the n th retransmission, the RRH sends feedback to the UE according to the rule $P_e(r, k, \mathcal{H}_n) \leq_{\text{NAK}}^{\text{ACK}} P_{\text{th}}$. Due to the monotonicity of the probability $P_e(r, k, \mathcal{H}_n)$ as a function of each eigenvalue, we have that the probability $P_e(r, k, \mathcal{H}_n)$ is no larger than $P_e(r, k, \mathcal{H}_{n-1})$. Therefore, similar to CC, we can calculate

$$P(D_n | \text{ACK}_n) = 1 - E[P_e(r, k, \mathcal{H}_n) | \mathcal{A}(P_{\text{th}})] \quad (32)$$

$$\text{and } P(\text{NAK}_n) = P(P_e(r, k, \mathcal{H}_n) > P_{\text{th}}), \quad (33)$$

where we have defined the event $\mathcal{A}(P_{\text{th}}) = \{P_e(r, k, \mathcal{H}_{n-1}) > P_{\text{th}}\} \cap \{P_e(r, k, \mathcal{H}_n) \leq P_{\text{th}}\}$. For the SISO case, we can calculate these quantities as

$$\begin{aligned} P(D_n | \text{ACK}_n) &= 1 - \frac{1}{\Delta(P_{\text{th}})} \int_0^\infty \cdots \int_0^\infty P_e(r, k, \text{diag}([\sqrt{x_1}, \dots, \sqrt{x_n}])) \\ &\quad \mathbf{1}(\mathcal{A}(P_{\text{th}})) \prod_{i=1}^n f_{\chi_2^2}(x_i) dx_1 \cdots dx_n \\ \text{and } P(\text{NAK}_n) &= \int_0^\infty \cdots \int_0^\infty \mathbf{1}(P_e(r, k, \text{diag}([\sqrt{x_1}, \dots, \sqrt{x_n}])) > P_{\text{th}}) \prod_{i=1}^n f_{\chi_2^2}(x_i) dx_1 \cdots dx_n, \end{aligned} \quad (34)$$

where

$$\Delta(P_{\text{th}}) = \int_0^\infty \cdots \int_0^\infty \mathbf{1}(\mathcal{A}(P_{\text{th}})) \prod_{i=1}^n f_{\chi_2^2}(x_i) dx_1 \cdots dx_n. \quad (35)$$

VI. ANALYSIS OF USER-CENTRIC LOW-LATENCY LOCAL FEEDBACK FOR C-RAN

In this section, we turn to the analysis of the user centric low-latency local feedback schemes introduced in Sec. III-B for C-RAN. Throughout, we focus on HARQ-IR for its practical relevance, see, e.g., [14]. Furthermore, we consider the case where each RRH has only one receiving antenna, i.e., $m_{r,l} = 1$ for $l = 1, \dots, L$. Extensions to other HARQ protocols and to scenarios with large number of antennas at the RRHs are possible by following similar arguments as in the previous sections and will not be further discussed here. We recall that in a C-RAN with local feedback, the retransmission decisions are made at the UE based on feedback from the RRHs. We treat separately the case of ideal zero-delay feedback from the BBU, and the hard and soft feedback schemes in the following.

A. Ideal Feedback

We first consider for reference the case of zero-delay ideal feedback from the BBU. Since the BBU jointly processes all the received signals for decoding, at the n th retransmission, the signal available at the BBU can be written, using (1), as $\mathbf{y}^n = [\mathbf{y}_1^T, \dots, \mathbf{y}_n^T]^T$, where

$$\mathbf{y}_n = \sqrt{\frac{s}{m_t}} \mathbf{H}_n \mathbf{x}_n + \mathbf{w}_n, \quad (36)$$

with $\mathbf{H}_n = [\mathbf{h}_{1,n}^T \mathbf{h}_{2,n}^T \dots \mathbf{h}_{L,n}^T]^T$ and $\mathbf{w}_n = [w_{1,n} \ w_{2,n} \dots w_{L,n}]^T$. We emphasize that we denoted here as $\mathbf{h}_{l,n}$ instead of $\mathbf{H}_{l,n}$ the vector containing the channel coefficients between the UE and l th RRH in the n th retransmission, so as to stress the focus on single-antenna RRHs. The effective received signal is hence given by

$$\mathbf{y}^n = \sqrt{\frac{s}{m_t}} \mathcal{H}_n [\mathbf{x}_1^T \dots \mathbf{x}_n^T]^T + [\mathbf{w}_1^T \dots \mathbf{w}_n^T]^T, \quad (37)$$

with $\mathcal{H}_n = \text{diag}([\mathbf{H}_1, \dots, \mathbf{H}_n])$. Therefore, the decoding error probability at the n th transmission is given by $P_e(r, k, \mathcal{H}_n)$.

The C-RAN performance in terms of throughput and the probability of success under ideal feedback can be obtained following the discussion in Sec. IV by computing the probability $P(\text{RTX}_n)$ that a retransmission is required at the n th transmission attempt. This can be bounded similar to (30) as $P(\text{RTX}_n) \leq P(\bar{D}_n) = E[P_e(r, k, \mathcal{H}_n)]$.

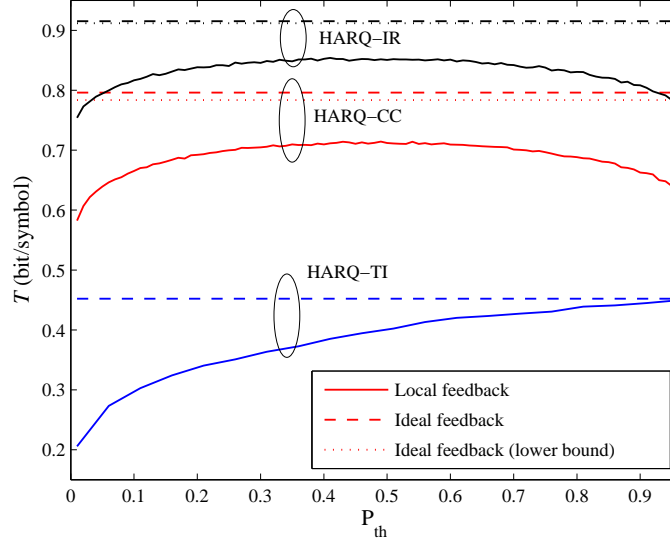


Fig. 6. Throughput versus threshold P_{th} for ideal feedback and local feedback in a D-RAN system ($s = 3$ dB, $n_{max} = 5$, $r = 2$ bit/symbol, $k = 50$, $m_t = 1$ and $m_r = 1$).

B. Hard Feedback Scheme

With the hard feedback low-latency scheme described in Sec. III-B1, each RRH calculates its own decoding error probability $P_e(r, k, \mathcal{H}_{l,n})$ with $\mathcal{H}_{l,n} = \text{diag}(\mathbf{h}_{l,1} \mathbf{h}_{l,2} \cdots \mathbf{h}_{l,n})$ and uses the rule (3), which reduces to

$$P_e(r, k, \mathcal{H}_{l,n}) \underset{\text{NAK}}{\overset{\text{ACK}}{\leq}} P_{th}. \quad (38)$$

Each RRH sends a single bit indicating the ACK/NAK feedback to the UE. The UE decides that a retransmission is necessary as long as all the RRHs return a NAK message, and it stops retransmission otherwise.

Throughput and probability of success can be computed as detailed in Sec. IV by using the following probabilities

$$P(D_n | \text{STOP}_n) = 1 - E \left[P_e(r, k, \mathcal{H}_n) \left| \prod_{l=1}^L \mathbf{1}(P_e(r, k, \mathcal{H}_{l,n}) > P_{th}) = 0 \right. \right] \quad (39)$$

$$\text{and } P(\text{RTX}_n) = P \left(\prod_{l=1}^L \mathbf{1}(P_e(r, k, \mathcal{H}_{l,n}) > P_{th}) = 1 \right). \quad (40)$$

The above probabilities can be calculated similar to the equations derived in Sec. V by averaging over the distribution of the eigenvalues of the involved channel matrices.

C. Soft Feedback Scheme

With the soft feedback introduced in Sec. III-B, each RRH quantizes the local CSI $\mathbf{h}_{l,n}$ with b bits. From the b feedback bits received from each RRH, the UE obtains the quantized channel vectors $\hat{\mathbf{h}}_{l,n}$ for $l \in \{1, \dots, L\}$. Based of these, the decision (4) is adopted, which reduces to

$$P_e(r, k, \hat{\mathcal{H}}_n) \underset{\text{RTX}}{\overset{\text{STOP}}{\leq}} P_{\text{th}}, \quad (41)$$

where $\hat{\mathcal{H}}_n = \text{diag}(\hat{\mathbf{H}}_1, \dots, \hat{\mathbf{H}}_n)$ and $\hat{\mathbf{H}}_n = [\hat{\mathbf{h}}_{1,n}^T \cdots \hat{\mathbf{h}}_{2,n}^T \cdots \hat{\mathbf{h}}_{L,n}^T]^T$ collect the quantized CSI. Accordingly, we can compute the desired probabilities as

$$P(D_n | \text{STOP}_n) = 1 - E[P_e(r, k, \mathcal{H}_n) | P_e(r, k, \hat{\mathcal{H}}_n) \leq P_{\text{th}}] \quad (42)$$

$$\text{and } P(\text{RTX}_n) = P(P_e(r, k, \hat{\mathcal{H}}_n) > P_{\text{th}}). \quad (43)$$

The above probabilities can be computed analytically or via Monte Carlo simulations by averaging over the distribution of the eigenvalues similar to Sec. V.

VII. NUMERICAL RESULTS AND DISCUSSION

In this section, we validate the analysis presented in the previous sections and provide insights on the performance comparison of ideal and local feedback schemes for D-RAN and C-RAN systems via numerical examples.

A. D-RAN

We first study the optimization of the threshold P_{th} used in the local feedback schemes. As an exemplifying case study, we consider the D-RAN strategy described in Sec. V. In Fig. 6 and Fig. 7, respectively, the throughput T and the probability of success P_s are shown versus P_{th} for $s = 3$ dB, $n_{\text{max}} = 5$ retransmissions, $r = 2$ bit/symbol and blocklength $k = 50$ for a SISO link, i.e., for $m_t = 1$ and $m_r = 1$. The curves have been computed using both the equations derived in Sec. V and Monte Carlo simulations. The latter refer to the simulation of the HARQ process in which the probability of error at the BBU is modeled by means of the Gaussian approximation. The analytical results are confirmed to match with the Monte Carlo simulations, except for the ideal feedback performance of HARQ-CC and HARQ-IR, for which, as discussed in Sec. V, the expressions (25) and (31) yield lower bounds on throughput and probability of success. As seen in the figures, the bounds are very accurate for k as small as 50.

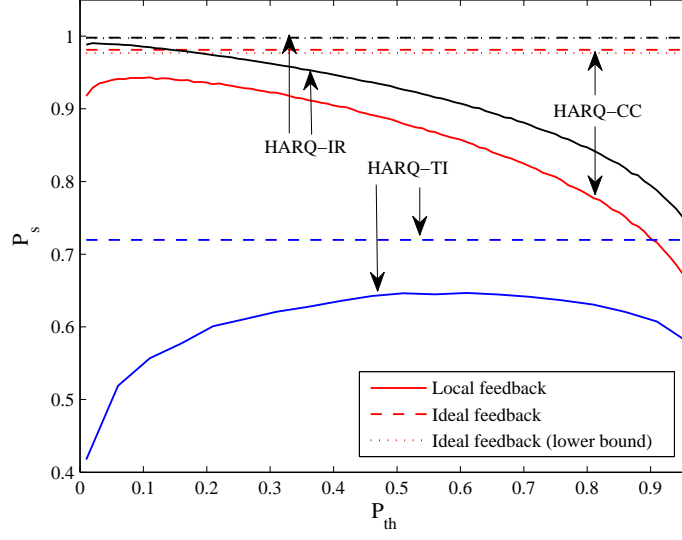


Fig. 7. Probability of success versus threshold P_{th} in a D-RAN system ($s = 3$ dB, $n_{max} = 5$, $r = 2$ bit/symbol, $k = 50$, $m_t = 1$ and $m_r = 1$).

From Fig. 6 and Fig. 7, it is also concluded that throughput and probability of success are maximized for different values of threshold P_{th} , with the throughput metric requiring a larger threshold. In fact, a larger value of P_{th} , while possibly causing the acknowledgement of packets that will be incorrectly decoded at the BBU, may enhance the throughput by allowing for the transmission of fresh information in a new HARQ session. This is particularly evident for HARQ-TI, for which setting $P_{th} = 1$ guarantees a throughput equal to the case of ideal feedback, but at the cost of a loss in the probability of success. It is also observed that more powerful HARQ schemes such as CC and IR are more robust to a suboptimal choice of P_{th} in terms of throughput, although lower values of P_{th} are necessary in order to enhance the probability of success by avoiding a premature transmission of an ACK message.

We now illustrate in Fig. 8 the throughput loss of local feedback as compared to the ideal feedback case, as a function of the blocklength k , for two rates $r = 1$ bit/symbol and $r = 3$ bit/symbol for HARQ-CC and HARQ-IR in a D-RAN system. Henceforth, to avoid clutter in the figures, we only show Monte Carlo results, given the match with analysis discussed above. The simulation are performed by setting $s = 4$ dB, $n_{max} = 10$ and we focus on a SISO link. For every value of k , the threshold P_{th} is optimized to maximize the throughput T under the constraint that the probability of success satisfies the requirement $P_s > 0.99$ (see, e.g., [14] and [21]). It

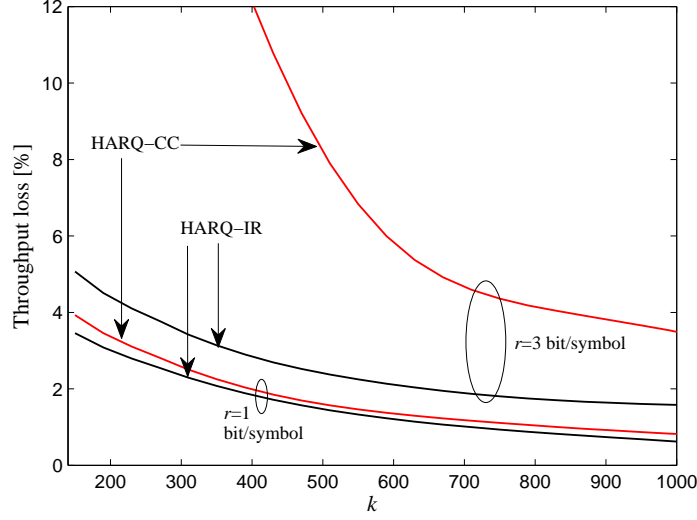


Fig. 8. Throughput loss versus blocklength k for HARQ-CC and HARQ-IR in a D-RAN system ($s = 4$ dB, $n_{max} = 10$, $m_t = 1$, $m_r = 1$, $P_s > 0.99$ for $r = 1$ bit/symbol and $r = 3$ bit/symbol).

can be seen that, as the blocklength increases, the performance loss of local feedback decreases significantly. This reflects a fundamental insight: The performance loss of local feedback is due to the fact that the local decisions are taken by the RRH based only on channel state information, without reference to the specific channel noise realization that affects the received packet. Therefore, as the blocklength k increases, and hence as the errors due to atypical channel noise realizations become less likely, the local decisions tend to be consistent with the actual decoding outcomes at the BBU. In other words, as the blocklength k grows larger, it becomes easier for the RRH to predict the decoding outcome at the BBU: In the Shannon regime of infinite k , successful or unsuccessful decoding depends deterministically on whether the rate r is above or below capacity.

A related conclusion can be reached from Fig. 9, where we investigate the throughput for MIMO ($m_t = m_r = m$), MISO ($m_t = m$ and $m_r = 1$) and SIMO ($m_t = 1$ and $m_r = m$) links versus the number of antennas m for HARQ-IR, with $s = 1$ dB, $n_{max} = 10$, $r = 5$ bit/symbol, $k = 100$. As in Fig. 8, the threshold P_{th} is optimized here, and henceforth, to maximize the throughput under the constraint $P_s > 0.99$. As m grows large, it is seen that the throughput of SIMO and MIMO increases significantly, while, at the same time, the throughput loss of the local feedback decreases. This is due to the fact that increasing the number of receive antennas effectively boosts the received SNR and hence reduces the impact of the noise on the decoding

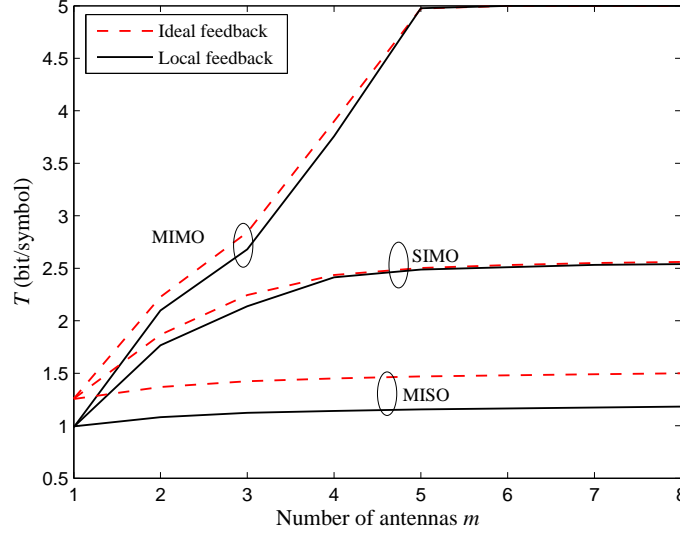


Fig. 9. Throughput versus the number of antennas for MISO, SIMO and MIMO with HARQ-IR in a D-RAN system ($s = 1$ dB, $n_{max} = 10$, $r = 5$ bit/symbol, $k = 100$ and $P_s > 0.99$).

outcome. This is unlike the case with MISO, since an increase in the number of transmit antennas only enhances the diversity order but does not improve the average received SNR.

B. C-RAN

We now turn our attention to the performance of low-latency local feedback for HARQ over C-RAN systems with $L > 1$ single-antenna RRHs and $m_t = 4$ antennas at the UE. Throughout, we consider the throughput of local feedback based on hard or soft feedback, under the constraint $P_s > 0.99$ on the probability of success. As a reference, we also consider the performance of a D-RAN system, i.e., with $L = 1$, under both ideal and local feedback (we mark the latter as “hard feedback” following the discussion in Sec. VI-B).

For soft feedback, we set different values for the number of feedback bits b , including $b = \infty$, with the latter being equivalent to a D-RAN system with three co-located antennas at the RRH (i.e., $m_{r,1} = 3$ and $L = 1$). We use a vector quantizer for each RRH l , in which $b' \leq b$ bits are used to quantize the channel direction $\mathbf{h}_{l,n}/\|\mathbf{h}_{l,n}\|$ and $b - b'$ bits for the amplitude $\|\mathbf{h}_{l,n}\|$. For vector quantization, we generate randomly quantization codebooks with normalized columns (see, e.g., [15]) until finding one for which the constraint on the probability of success is met. The amplitude $\|\mathbf{h}_{l,n}\|$ of each channel vector is quantized with the remaining $b' - b$ using a quantizer with numerically optimized thresholds. For $b = 3$, $b = 6$, $b = 9$ and $b = 16$, the

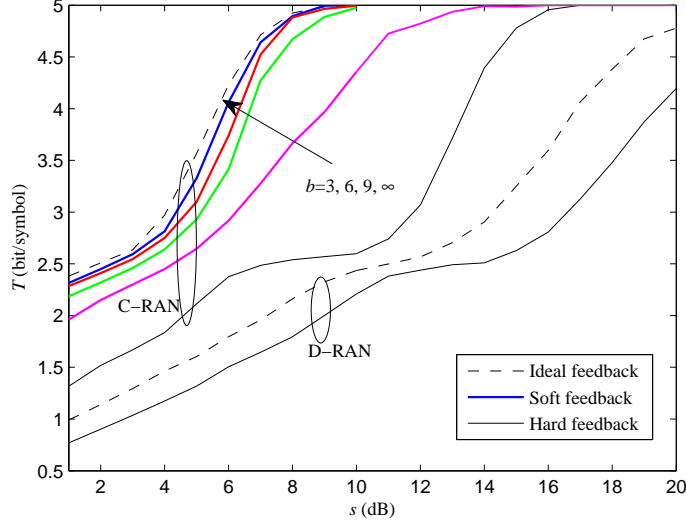


Fig. 10. Throughput versus SNR s for D-RAN ($L = 1$) and C-RAN ($L = 3$) systems ($n_{max} = 10$, $r = 5$ bit/symbol, $k = 100$, $P_s > 0.99$, $m_t = 4$, $m_{r,l} = 1$).

number of bits used for the quantization of the direction of each channel vector are $b' = 1$, $b' = 4$, $b' = 5$ and $b' = 12$.

In Fig. 10, the throughput of the schemes outlined above is shown versus the SNR parameter s . We first observe that hard feedback, which only require 1 bit of feedback per RRH, is able to improve over the performance of D-RAN, but the throughput is limited by the errors due to the user-centric local decisions based on partial feedback from the RRHs. This limitation is partly overcome by implementing the soft feedback scheme, whose throughput increases for a growing feedback rate. Note that, even with an infinite feedback rate, the performance of local feedback still exhibits a gap as compared to ideal feedback for the same reasons discussed above for D-RAN systems. Also, the flattening of the throughput of less performing schemes around $T = 2.5$ for intermediate SNR levels is due to the need to carry out at least two retransmissions unless the SNR is sufficiently large (see, e.g., [22]).

We finally show in Fig. 11 the throughput of ideal and soft feedback schemes versus the blocklength k for a C-RAN system with $L = 2$ and $L = 3$. We observe that, in a C-RAN system with a sufficiently small feedback rate such as $b = 3$ and $b = 6$, an increase in the blocklength k does not significantly increase the throughput, which is limited by the CSI quantization error. However, with a larger b , such as $b = 16$, the throughput can be more significantly improved

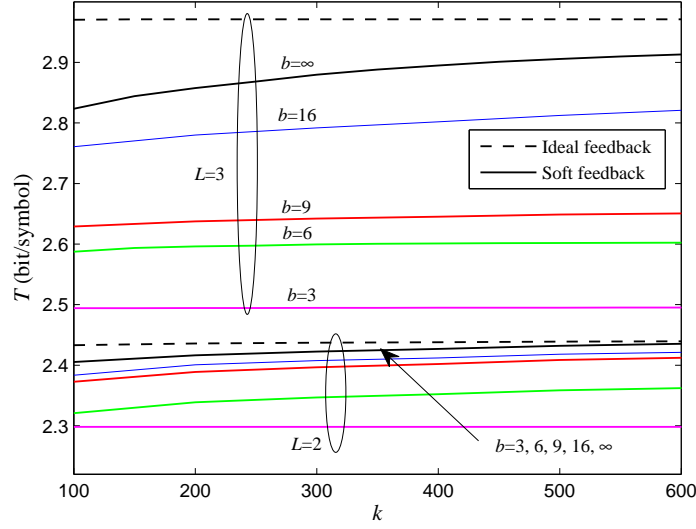


Fig. 11. Throughput versus blocklength k for hard and soft feedback schemes in C-RAN with $L = 3$ and $L = 2$. The throughput of the hard feedback scheme for $L = 2$ and $L = 3$ (not shown) are $T = 1.7$ and $T = 1.77$, respectively ($s = 4$ dB, $n_{max} = 10$, $r = 5$ bit/symbol, $P_s > 0.99$, $m_t = 4$, $m_{r,l} = 1$).

towards the performance of ideal feedback, especially for a smaller number of RRHs.

VIII. CONCLUDING REMARKS

The performance of D-RAN and C-RAN systems is currently under close scrutiny as limitations due to constraints imposed by fronthaul capacity and latency are increasingly brought to light (see, e.g., [1]). An important enabling technology to bridge the gap between the desired lower cost and higher spectral efficiency of D-RAN and C-RAN and its potentially poor performance in terms of throughput at higher layers is the recently proposed control and data separation architecture [10]. In this context, this work has considered D-RAN and C-RAN systems in which retransmission decisions are made at the edge of the network, that is, by the RRHs or UEs, while data decoding is carried out in a centralized fashion at the BBUs.

As shown, for D-RAN, this class of solutions has the potential to yield throughput values close to those achievable with ideal zero-delay feedback from the BBUs, particularly when the packet length is sufficiently long or the number of received antennas is large enough. For C-RAN, it was argued that multi-bit feedback messages from the RRHs are called for in order to reduce the throughput loss and a specific scheme based on vector quantization was proposed to this end.

Interesting future work include the analysis of control and data separation architectures for C-RAN systems for the purpose of user detection activity in random access in scenarios with a massive number of devices.

REFERENCES

- [1] China Mobile Research Institute, “C-RAN: The road towards green RAN, white paper,” 2010. [Online]. Available: http://labs.chinamobile.com/cran/wp-content/uploads/CRAN_white_paper_v2_5_EN.pdf.
- [2] A. Checko, H. Christiansen, Y. Yan, L. Scolari, G. Kardaras, M. Berger, and L. Dittmann, “Cloud RAN for mobile networks-a technology overview,” *IEEE Commun. Surveys Tuts.*, vol. 17, no. 1, pp. 405–426, First quarter 2015.
- [3] M. Nahas, A. Saadani, J. Charles, and Z. El-Bazzal, “Base stations evolution: Toward 4G technology,” in *Proc. Int. Conf. on Telecommunications (ICT)*, pp. 1-6, Aalborg, Denmark, Apr. 2012.
- [4] NGMN Alliance, “Further study on critical C-RAN technologies, White paper,” 2015. [Online]. Available: https://www.ngmn.org/uploads/media/NGMN_RANEV_D2_Further_Study_on_Critical_C-RAN_Technologies_v1.0.pdf.
- [5] A. Cipriano, P. Gagneur, G. Vivier, and S. Sezginer, “Overview of ARQ and HARQ in beyond 3G systems,” in *Proc. IEEE Int. Symp. on Personal, Indoor and Mobile Radio Communications (PIMRC)*, pp. 424-429, Istanbul, Turkey, Sep. 2010.
- [6] U. Dötsch, M. Doll, H.-P. Mayer, F. Schaich, J. Segel, and P. Sehier, “Quantitative analysis of split base station processing and determination of advantageous architectures for LTE,” *Bell Labs Technical Journal*, vol. 18, no. 1, pp. 105–128, Jun. 2013.
- [7] Q. Han, C. Wang, M. Levorato, and O. Simeone, “On the effect of fronthaul latency on ARQ in C-RAN systems.” [Online]. Available: <http://arxiv.org/abs/1510.07176>
- [8] D. Wubben, P. Rost, J. Bartelt, M. Lalam, V. Savin, M. Gorgoglione, A. Dekorsy, and G. Fettweis, “Benefits and impact of cloud computing on 5G signal processing: Flexible centralization through Cloud-RAN,” *IEEE Signal Process. Mag.*, vol. 31, no. 6, pp. 35–44, Nov. 2014.
- [9] A. De La Oliva, X. Costa Perez, A. Azcorra, A. Di Giglio, F. Cavaliere, D. Tiegelbekkers, J. Lessmann, T. Haustein, A. Mourad, and P. Iovanna, “Xhaul: toward an integrated fronthaul/backhaul architecture in 5G networks,” *IEEE Wireless Commun.*, vol. 22, no. 5, pp. 32–40, Oct. 2015.
- [10] A. Mohamed, O. Onireti, M. Imran, A. Imran, and R. Tafazolli, “Control-data separation architecture for cellular radio access networks: A survey and outlook,” *to appear in IEEE Commun. Surveys Tuts.*, 2015.
- [11] P. Rost and A. Prasad, “Opportunistic hybrid ARQ-enabler of centralized-RAN over nonideal backhaul,” *IEEE Wireless Commun. Letters*, vol. 3, no. 5, pp. 481–484, Oct. 2014.
- [12] Y. Polyanskiy, H. Poor, and S. Verdú, “Channel coding rate in the finite blocklength regime,” *IEEE Trans. Inf. Theory*, vol. 56, no. 5, pp. 2307–2359, May 2010.
- [13] Y. Polyanskiy, “Channel coding: non-asymptotic fundamental limits.” Ph.D. thesis, Princeton university, 2010.
- [14] E. Dahlman, S. Parkvall, J. Skold, P. Bemin, *3G Evolution: HSPA and LTE for Mobile Broadband*. Academic Press, second edition, 2008.
- [15] D. Love, R. Heath, and T. Strohmer, “Grassmannian beamforming for multiple-input multiple-output wireless systems,” *IEEE Trans. Inf. Theory*, vol. 49, no. 10, pp. 2735–2747, Oct. 2003.
- [16] G. Caire and D. Tuninetti, “The throughput of hybrid-ARQ protocols for the Gaussian collision channel,” *IEEE Trans. Inf. Theory*, vol. 47, no. 5, pp. 1971–1988, Jul. 2001.
- [17] W. Yang, G. Durisi, T. Koch, and Y. Polyanskiy, “Quasi-static MIMO fading channels at finite blocklength.” [Online]. Available: <http://arxiv.org/abs/1311.2012>.

- [18] P. Frenger, S. Parkvall, and E. Dahlman, "Performance comparison of HARQ with chase combining and incremental redundancy for HSDPA," in *Proc. IEEE Vehicular Technology Conference (VTC)*, vol. 3, pp. 1829–1833, Atlantic City, New Jersey, USA, Oct. 2001.
- [19] A. M. Tulino and S. Verdú, *Random Matrix Theory and Wireless Communications*. Now Publishers Inc, 2004.
- [20] R. Sassioui, E. Pierre-Doray, L. Szczecinski, B. Pelletier, "Modelling decoding errors in HARQ." [Online]. Available: <http://arxiv.org/abs/1512.02511>
- [21] A. Lozano and N. Jindal, "Are yesterday's information-theoretic fading models and performance metrics adequate for the analysis of today's wireless systems?" *IEEE Commun. Mag.*, vol. 50, no. 11, pp. 210–217, Nov. 2012.
- [22] I. Stanojev, O. Simeone, and Y. Bar-Ness, "Performance analysis of collaborative hybrid-ARQ incremental redundancy protocols over fading channels," in *Proc. IEEE Signal Processing Advances in Wireless Communications (SPAWC)*, pp. 1–5, Cannes, France, Jul. 2006.